PHILOSOPHICAL TRANSACTIONS OF THE ROYAL SOCIETY A MATHEMATICAL, PHYSICAL & ENGINEERING SCIENCES

Rotational and Vibronic Structure in the Electronic Spectra of Linear Open-Shell Cations [and Discussion]

J. P. Maier, E. Hirota and G. Duxbury

Phil. Trans. R. Soc. Lond. A 1988 **324**, 209-221
doi: 10.1098/rsta.1988.0012

Phil. Trans. R. Soc. Lond. A **324**, 209–221 (1988)
Printed in Great Britain

Rotational and vibronic structure in the electronic spectra of linear open-shell cations

By J. P. Maier

Institut für Physikalische Chemie, Universität Basel, Klingelbergstrasse 80, *CH*-4056 *Basel, Switzerland*

The vibrational and rotational structure of the electronic transitions of open-shell cations of linear polyatomics has been studied by three complementary techniques. In one, the emission spectra of ions of unstable species, XCP$^+$ and XBS$^+$, with X = H, D and F, are obtained by electron-impact excitation on effusive and supersonic free jets. The vibronic structure of their $\tilde{A}^2\Sigma^+ \rightarrow \tilde{X}^2\Pi_i$ band systems could be analysed. The changes and distinct features of the rotational profiles at low rotational temperatures in the emission spectra of diacetylene cation have been used to establish the absolute numbering in the rotational analysis of the $\tilde{A}^2\Pi_u$–$\tilde{X}^2\Pi_g$ transition. The second approach is based on the measurement of the laser excitation spectra of ions and has been used to confirm the vibrational assignment of complex emission spectra, such as the $\tilde{B}^2\Pi \rightarrow \tilde{X}^2\Pi$ transition of ClCN$^+$, and to resolve the rotational structure in the $\tilde{A}^2\Pi_{\frac{3}{2}} \leftarrow \tilde{X}^2\Pi_{\frac{3}{2}}$ transitions of the haloacetylene cations XCCH$^+$, X = Cl, Br, I. The most recent development is the demonstration that the stimulated emission pumping approach can be used to probe the electronic structure of ions in a flow system.

1. Introduction

Electronic spectroscopy has a long-standing tradition of providing information on the structure and spectroscopic parameters for transient species (Herzberg 1971). Many radicals and diatomic ions were thus characterized, initially by using classical absorption and emission approaches, and subsequently further and finer details have been discovered by laser techniques (Herzberg 1985). As far as polyatomic cations are concerned, the application of laser-based methods is even more recent (Miller & Bondybey 1982). However, following the identification of the emission spectra of over a hundred open-shell organic cations in the gas phase generated by electron-beam excitation (Maier 1980), higher resolution and state-selected investigations could be undertaken (Maier 1982).

Our research interests in the last years have focused on the spectroscopic characterization of polyatomic open-shell cations by emission spectroscopy with supersonic free jets, by laser excitation of the fluorescence and absorption measurements in neon matrices (Maier 1986). The present article gives examples of some of the recently completed studies with the first two techniques to obtain new vibronic data on triatomic cations of unstable molecules, to resolve the rotational structure in the electronic transitions of substituted acetylene cations and to use the techniques hand-in-hand to provide unambiguous vibronic and rotational assignments. Additionally, the stimulated emission pumping technique has also been demonstrated to be a viable approach to probe the ground state of ions.

2. Emission spectroscopy

Electron-impact excitation of the emission spectra has proved to be a valuable method in the studies of polyatomic cations in the gas phase, especially in obtaining the first set of data on their electronic transitions (Maier 1980). The incorporation of a seeded helium supersonic free jet as the source led to further progress in this area (Klapstein *et al.* 1983). This approach was consequently chosen to provide the initial information on the optical transitions of ions of unstable species, i.e. XCP^+, X = H, D, F and XBS^+, X = H, D, F, Cl. The molecular species themselves were produced by fast-flow methods from the appropriate precursors as described in their studies by microwave and infrared (IR) spectroscopy, and have also all been subjected to photoelectron spectroscopic investigations (Kroto 1982). The latter provided the first information on their ions, albeit at low resolution. Nevertheless, these data were important in assigning the observed emission-bands systems to the electronic transitions of such cations.

The $\tilde{A}^2\Sigma^+ \rightarrow \tilde{X}^2\Pi_i$ emission-band systems of phosphorus substituted alkyne ions XCP^+, with X = H, D (King *et al.* 1981), F (King *et al.* 1984*a*), and of the related thioborines XBS^+, with X = H, D (King *et al.* 1985*a*), F and Cl (King *et al.* 1986), have thus been obtained by electron-impact excitation. Following the preliminary vibrational analyses, and for HCP^+ and DCP^+ also rotational analyses (King *et al.* 1982), the most recent studies have been focused on understanding the complex vibronic pattern in the spectra of HCP^+ and DCP^+ (King *et al.* 1987). To this end, the emission spectra have been recorded with improved signal:noise ratios in the relevant regions, and especially helpful have been the changes in the rotational profiles at low rotational temperatures attained by means of a seeded helium supersonic free jet. This is especially the case for the weaker bands for which the resolution of the rotational structure proved not to be possible. In addition, the drastic narrowing of the bands led to the detection of weak transitions (which are often obscured at higher temperatures), such as those associated with single and double quantum excitation of the ground-state ($\tilde{X}^2\Pi_i$) bending mode, ν_2''.

As an example, the spectral region near the origin bands of the $\tilde{A}^2\Sigma^+ \rightarrow \tilde{X}^2\Pi_i$ transition of HCP^+ is shown in figure 1 with rotational temperatures of *ca.* 300 K (upper) and 20–30 K (bottom trace). The latter temperature is inferred by simulation of the profiles from the known rotational constants (King *et al.* 1982). The two spin–orbit components are seen ($A'' \sim -150\ cm^{-1}$) and at *ca.* 300 K the P-head as well as the stronger Q-branch head are distinct. On cooling, however, the P-head disappears. Thus a comparison of two such spectra enables the high and low J transitions to be distinguished. Furthermore, the R-branches are more intense than the P-branches for the $\Omega = \frac{1}{2}$ component bands but equally strong for $\Omega = \frac{3}{2}$ ones. All these features have been used as a diagnostic tool in the assignments.

The excitation of the degenerate ν_2 mode is identified by means of sequence transitions, e.g. 010–010, as well as even quanta progressions, e.g. 000–020. The discernible band systems are complicated by a combination of Renner and Fermi interactions (see figure 2). An analysis has proved possible in terms of the parameters used to describe such phenomena e.g. $\epsilon\omega_2'' \sim -26.5$ $(-18.7)\ cm^{-1}$, $g_\kappa'' = 6.4$ $(3.6)\ cm^{-1}$ for the Renner effect in HCP^+ (DCP^+). Though some discrepancies remain, the essential spectral features are mimicked (King *et al.* 1987).

Vibronic analyses to such detail have also been completed for the $\tilde{A}^2\Sigma^+ \rightarrow \tilde{X}^2\Pi_i$ transitions of HBS^+ and DBS^+, and to a more limited extent for FCP^+ and recently FBS^+ and $ClBS^+$. In table 1 are summarized the pertinent spectroscopic data deduced for the XCP^+ and XBS^+ ions. In view of this information, it should in due course be feasible to obtain further and more precise data by methods based on laser excitation.

PHILOSOPHICAL TRANSACTIONS OF THE ROYAL SOCIETY A MATHEMATICAL, PHYSICAL & ENGINEERING SCIENCES

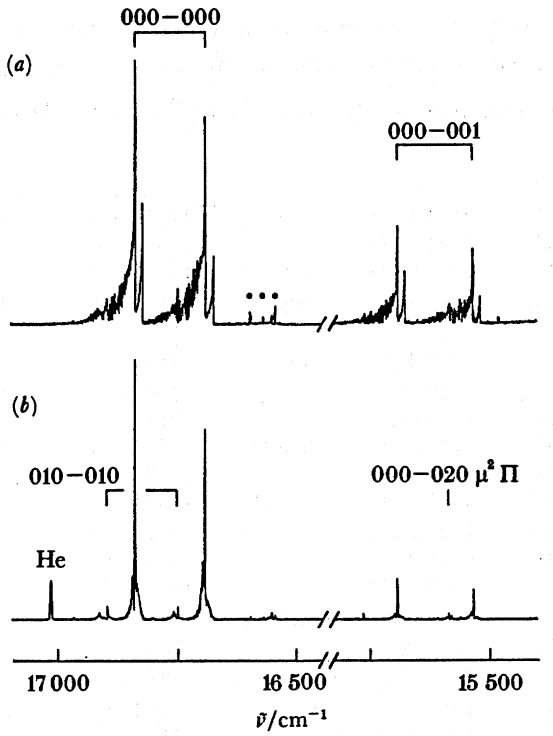

FIGURE 1. Two spectral regions in the $\tilde{A}^2\Sigma^+ \rightarrow \tilde{X}^2\Pi_i$ emission system of HCP^+ recorded (0.065 nm FWHM) with electron impact excitation on an effusive beam of pure HCP (top) and on a seeded helium supersonic free jet (bottom).

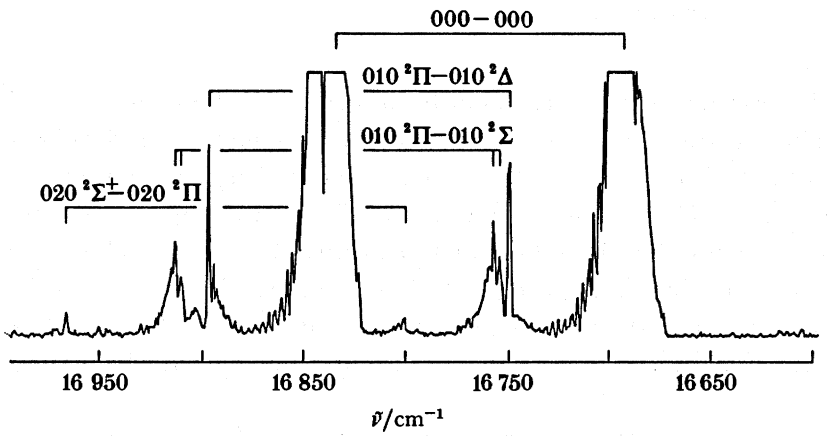

FIGURE 2. Expanded scan of the spectral features adjoining the origin bands in the $\tilde{A}^2\Sigma^+ \rightarrow \tilde{X}^2\Pi_i$ emission spectrum of supersonically cooled HCP^+.

For the $\tilde{A}^2\Pi_u \rightarrow \tilde{X}^2\Pi_g$ transition of the diacetylene cation, the pronounced changes in the band profiles on cooling enable the absolute numbering in the rotational analysis to be established. Although the emission spectrum was identified and rotationally analysed a long time ago (Callomon 1956), in fact two physically reasonable numberings were obtained (and hence two sets of spectroscopic constants). This ambiguity was resolved by the following procedure.

In figure 3 are shown two recordings of the origin band of the $\tilde{A}^2\Pi_{u,\Omega} \rightarrow \tilde{X}^2\Pi_{g,\Omega}$ ($\Omega = \frac{3}{2}, \frac{1}{2}$)

TABLE 1. VIBRATIONAL FREQUENCIES (RECIPROCAL CENTIMETRES) OF THE PHOSPHAETHYNE AND SULPHIDOBORON CATIONS INFERRED FROM THEIR $\tilde{A}^2\Sigma^+ \rightarrow \tilde{X}^2\Pi_i$ EMISSION SPECTRA

(Also are given the apparent spin–orbit splittings, $A_{0,\mathrm{eff}}(\mathrm{cm}^{-1})$ in the $\tilde{X}^2\Pi_i$ state. The references to the studies are to be found in the text.)

ion	state	ν_1	ν_2	ν_3	$A_{0,\mathrm{eff}}$
HCP^{+a}	$\tilde{X}^2\Pi_{\frac{3}{2}}$	3125.1 (4)	642 (1)	1147.1 (4)	−146.97 (3)
	$^2\Pi_{\frac{1}{2}}$	3124.9 (4)		1159.9 (4)	
	$\tilde{A}^2\Sigma^+$	2985.6 (4)	706 (1)	1275.4 (4)	
DCP^{+b}	$\tilde{X}^2\Pi_{\frac{3}{2}}$	2356.5 (4)	499 (1)	1112.4 (4)	−146.71 (1)
	$^2\Pi_{\frac{1}{2}}$	2356.6 (4)		1113.4 (4)	
	$\tilde{A}^2\Sigma^+$	2274.4 (4)	552 (1)	1218.1 (4)	
FCP^+	$\tilde{X}^2\Pi_i$	1729 (2)		765 (1)	−190.2 (6)
	$\tilde{A}^2\Sigma^+$	1866 (2)		817 (2)	
$H^{11}B^{32}S^{+c}$	$\tilde{X}^2\Pi_{\frac{3}{2}}$	2746.8 (4)	659 (1)	975.9 (4)	−322.6 (4)
	$^2\Pi_{\frac{1}{2}}$	2747.1 (4)		~991[d]	
	$\tilde{A}^2\Sigma^+$	2214.8 (4)	550 (1)	1050.9 (4)	
$D^{11}B^{32}S^+$	$\tilde{X}^2\Pi_{\frac{3}{2}}$	2071.1 (4)		937.4 (4)	−322.2 (4)
	$^2\Pi_{\frac{1}{2}}$	2074.2 (4)		~993[d]	
	$\tilde{A}^2\Sigma^+$	1706.6 (4)		1011.1 (4)	
$F^{11}B^{32}S^+$	$\tilde{X}^2\Pi_{\frac{3}{2}}$	1721 (2)	339 (2)	637 (2)	−339 (2)
	$^2\Pi_{\frac{1}{2}}$	1718 (2)		633 (2)	
	$\tilde{A}^2\Sigma^+$	1718 (2)		691 (2)	
$^{35}Cl^{11}B^{32}S^+$	$\tilde{X}^2\Pi_i$	1347.8 (8)		508.9 (8)	−383 (1)
	$\tilde{A}^2\Sigma^+$	1390.6 (8)		516.0 (8)	

[a] $B_0(\tilde{X}^2\Pi_i) = 0.6224\ (16)$; $B_0(\tilde{A}^2\Sigma^+) = 0.6690\ (17)\ \mathrm{cm}^{-1}$.
[b] $B_0(\tilde{X}^2\Pi_i) = 0.5284\ (2)$; $B_0(\tilde{A}^2\Sigma^+) = 0.5682\ (2)\ \mathrm{cm}^{-1}$.
[c] $B_0(\tilde{X}^2\Pi_i) = 0.5760\ (2)$; $B_0(\tilde{A}^2\Sigma^+) = 0.6148\ (2)\ \mathrm{cm}^{-1}$. These values are taken from McDonald & Innes (1969), where they are erroneously attributed to BS.
[d] Estimated from combination bands.

transition of diacetylene cation in emission from a seeded helium supersonic free jet (Kuhn *et al.* 1986). The top trace corresponds to a rotational temperature of *ca.* 10 K whereas the bottom one corresponds to 70–90 K. At the latter (and higher) temperature, the two R-heads are prominent and the Q_1-branch is barely perceptible; on the other hand, the Q_1-branch is the most distinct one at reduced rotational temperatures. The Q_2-branch is still not discernible because its intensity is nine times lower according to the Ω^2-dependence in the line strength. This difference then allows the unambiguous identification of the R_1- and R_2-heads, showing in this case that $|A''| > |A'|$ by *ca.* 3.3 cm^{-1}, both spin-orbit constants being negative (inverted states).

Although the present emission spectra were recorded at relatively low resolution (0.25 cm^{-1} FWHM), the position of the Q_1-branch maximum is located to within ± 0.05 cm^{-1} and establishes the correct numbering. From the two possible sets of spectroscopic constants derived from the rotational analysis the position of the $Q_1(J = 1.5)$ line is calculated. Whereas one of the values agrees exactly with the observation (see the middle trace of figure 3), also in the case of the corresponding data and spectrum of dideuterodiacetylene cation, the other value lies 0.3 cm^{-1} to higher energy. The correct numbering is thus established. The spectroscopic constants were also newly determined for both diacetylene and dideuterodiacetylene cations by fitting simultaneously the line positions in their $\tilde{A}^2\Pi_u \leftarrow \tilde{X}^2\Pi_g$ laser excitation spectra to the eigenvalues of the usual hamiltonian matrix. The derived B_0'', B_0' values are included in the compilation of table 2.

PHILOSOPHICAL TRANSACTIONS OF THE ROYAL SOCIETY A MATHEMATICAL, PHYSICAL & ENGINEERING SCIENCES

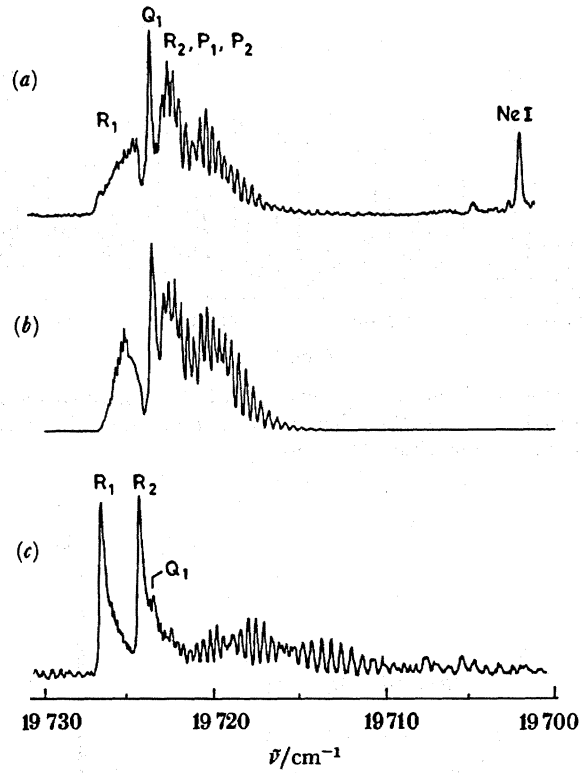

FIGURE 3. The origin band in the $\tilde{A}^2\Pi_u \rightarrow \tilde{X}^2\Pi_g$ emission spectrum of diacetylene cation obtained at 0.25 cm^{-1} resolution with electron impact on a supersonic expansion of diacetylene seeded in helium. Traces (*a*) and (*c*) correspond to rotational temperatures of 10 K and 70–90 K respectively. The middle trace (*b*) is a computer simulation of the transition (see text), $T = 10$ K.

3. LASER EXCITATION SPECTROSCOPY

The advantage of using emission and laser excitation spectroscopies in tandem for the spectral characterization of open-shell cations is illustrated by two examples. In the first, the vibrational analysis of the laser excitation spectrum of chlorocyanide cation was needed to locate the origin of the transition, which in turn enabled the emission spectrum to be interpreted. In the second, the initial information provided by the emission data on the haloacetylene cations led to the study of these species at higher resolution by laser excitation, and subsequently to the IR rotational and related spectroscopic constants.

In figure 4 is shown the main part of the $\tilde{B}^2\Pi_i \rightarrow \tilde{X}^2\Pi_i$ emission spectrum of rotationally cooled ($T_{rot} = 5$–10 K) chlorocyanide cation excited in a seeded supersonic free jet (Fulara *et al.* 1985). Although the spectrum is much improved compared to that with an effusive source (Allan & Maier 1976), several vibronic assignments of the band system appear to be possible. The complex vibration pattern arises from the large geometry change taking place on passing from the $\tilde{X}^2\Pi$ to the $\tilde{B}^2\Pi$ ionic state (mainly an increase in the C–Cl distance) as well as from the strong overlap of the $^2\Pi_{\frac{3}{2}} \rightarrow {}^2\Pi_{\frac{3}{2}}$ and $^2\Pi_{\frac{1}{2}} \rightarrow {}^2\Pi_{\frac{1}{2}}$ subsystems. However, the location of their origins is readily established by recording the laser excitation spectrum of this transition (Celii *et al.* 1986*a*). In the latter approach, the ions are prepared essentially all in the lowest vibrational level of the $\tilde{X}^2\Pi_i$ state by means of Penning ionization and collisional relaxation. Consequently the intensity of the origin band (of the $\Omega = \frac{3}{2}$ subsystem) becomes appreciable in

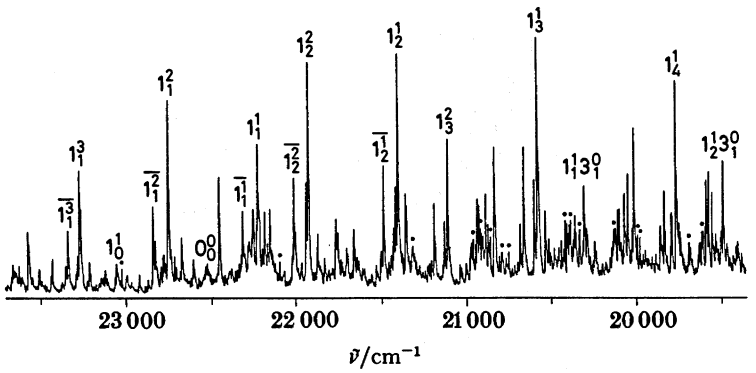

FIGURE 4. A portion of the $\tilde{B}^2\Pi \rightarrow \tilde{X}^2\Pi$ emission spectrum of $ClCN^+$ generated by electron impact on a seeded helium supersonic free jet (0.04 nm resolution). The horizontal bar above the vibrational assignment identifies the $\Omega = \frac{1}{2}$ system; atomic lines are marked with a dot.

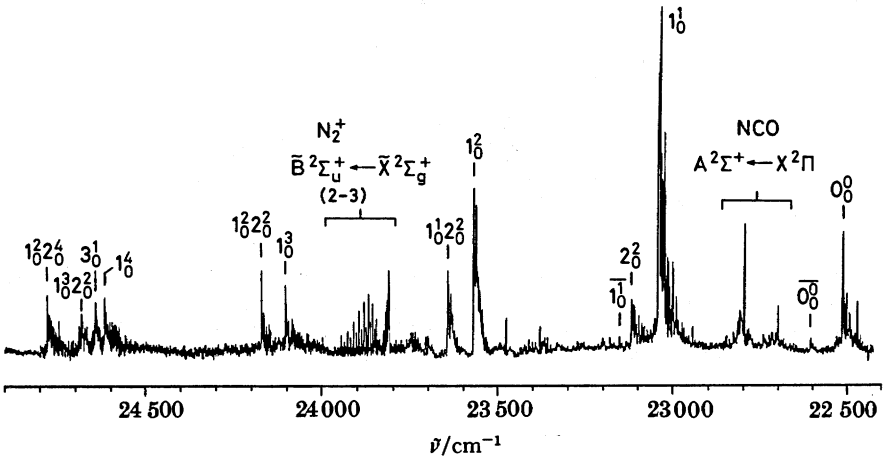

FIGURE 5. The main part of the $\tilde{B}^2\Pi \leftarrow \tilde{X}^2\Pi$ laser excitation spectrum of $ClCN^+$ recorded with a resolution of 0.2 cm^{-1}.

spite of the Franck–Condon factors (see figure 5). The origin band of the $\tilde{B}^2\Pi_{\frac{1}{2}} \leftarrow \tilde{X}^2\Pi_{\frac{1}{2}}$ subsystem is also apparent, but is rather weak as a result of the reduced population of the lower level because of collisional deactivation.

The combination of the information forthcoming from the excitation and emission (the $\tilde{A}^2\Sigma^+ \rightarrow \tilde{X}^2\Pi_i$ transition is also seen) experiments allows most of the features in the two spectra to be assigned and results in the determination of the vibrational frequencies of $^{35}ClCN^+$ and $^{37}ClCN^+$ in the $\tilde{X}^2\Pi_i$, $\tilde{A}^2\Sigma^+$ and $\tilde{B}^2\Pi_i$ states, as well as the spin–orbit constants. Most recently, the rotational structure of some of the bands has been resolved by using narrower laser bandwidth (*ca.* 0.04 cm^{-1}) excitation and the analysis of such data for various isotopically labelled derivatives of $ClCN^+$ leads to their rotational constants and r_s geometric structure (Celii *et al.* 1988). Complementary vibronic and rotational analyses have also been accomplished for the isotopes of $BrCN^+$ (Hanratty *et al.* 1988).

The haloacetylene cations, $XCCH^+$, have often featured as prototypes in the development of the spectroscopic techniques for open-shell cations. Following the detection of their $\tilde{A}^2\Pi_i \rightarrow \tilde{X}^2\Pi_i$ emission spectra by electron-impact excitation on an effusive beam (Allan *et al.* 1977), the vibronic analysis of this transition had to await the introduction of the supersonic

free jet and the laser excitation approaches before the complexity of the spectra could be disentangled (Maier 1986). In particular, in an analogous way to that illustrated above for $ClCN^+$, the $\tilde{A}^2\Pi_i \leftarrow \tilde{X}^2\Pi_i$ laser excitation spectra of $XCCH^+$, X = Cl, Br, I, recorded with moderate resolution (*ca.* 0.2 cm^{-1}) enabled the origins to be identified and this led, in turn, to vibrational analysis of the band systems. The vibrational frequencies are thus known to ± 1 cm^{-1} for most of the modes for these ions in their $\tilde{X}^2\Pi_i$ and $\tilde{A}^2\Pi_i$ states.

Resolution of the rotational structure in the laser excitation spectra of the haloacetylene cations $XCCH^+$, X = Cl (King *et al.* 1985*b*), Br (King *et al.* 1984*b*), and I (Maier & Ochsner 1985) followed, and the rotational and related spectroscopic constants have been evaluated. Because in all three haloacetylene cations only the $\tilde{A}^2\Pi_{\frac{3}{2}} \leftarrow \tilde{X}^2\Pi_{\frac{3}{2}}$ spin-orbit subsystem could be studied, the analyses yield the B_{eff} constants. These are collected in table 2 together with the B_0 values for the diacetylene cations obtained also by this approach from a simultaneous fit for $\Omega = \frac{3}{2}$ and $\frac{1}{2}$ components (Kuhn *et al.* 1986).

In figure 6 the rotationally resolved laser excitation spectrum of the 3_0^1 band of the $\tilde{A}^2\Pi_{\frac{3}{2}} \leftarrow \tilde{X}^2\Pi_{\frac{3}{2}}$ transition of iodoacetylene cation is reproduced (Maier & Ochsner 1985). The R- and P-branches are designated; the Q-branch is too weak to be detected at the ambient temperature 100–150 K employed in the measurements. The spectroscopic constants were determined by a least-squares fit between the line positions and those calculated from the differences of the eigenvalues of the upper- and lower-state hamiltonians. The effective closed-form expression used for the rotational energy levels,

$$F_v(J) = B_{\text{eff},v}([J+\tfrac{1}{2}]^2-1) - D_{\text{eff},v}([J+\tfrac{1}{2}]^2-2)^2,$$

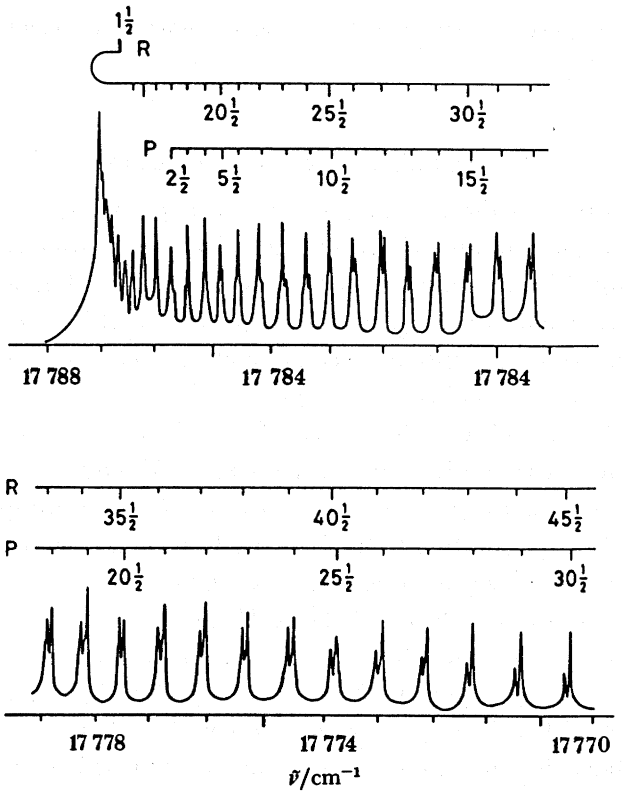

FIGURE 6. Rotationally resolved laser excitation spectrum (0.04 cm^{-1} FWHM) of the $\tilde{A}^2\Pi_{\frac{3}{2}} \leftarrow \tilde{X}^2\Pi_{\frac{3}{2}}$ 3_0^1 transition of the deuteroiodoacetylene cation.

is obtained by second-order perturbation theory from the published matrix elements (Zare *et al.* 1973). The determined rotational constant B_{eff} by this treatment is given in table 2 for the zeroth level of the $\tilde{X}^2\Pi$ and $\tilde{A}^2\Pi$ states of $ICCH^+$ and $ICCD^+$.

For the chloroacetylene and bromoacetylene cations, the presence of the naturally occurring halogen isotopes complicates the spectra on the one hand, but in return yields the partial r_s structure from the knowledge of the respective rotational constants.

TABLE 2. ROTATIONAL CONSTANTS (RECIPROCAL CENTIMETRES) FOR THE HALOACETYLENE AND DIACETYLENE CATIONS INFERRED FROM THE STRUCTURE IN THEIR $\tilde{A}^2\Pi_i \leftarrow \tilde{X}^2\Pi_i$ LASER EXCITATION SPECTRA[a]

cation	$B_{0,\text{eff}}$ $\tilde{X}^2\Pi_{\frac{3}{2}}$	$\tilde{A}^2\Pi_{\frac{3}{2}}$
$^{35}Cl{-}C{\equiv}C{-}H^+$	0.194647 (49)	0.170881 (48)
$^{37}Cl{-}C{\equiv}C{-}H^+$	0.191063 (60)	0.167680 (60)
$^{35}Cl{-}C{\equiv}C{-}D^+$	0.176968 (38)	0.156338 (37)
$^{37}Cl{-}C{\equiv}C{-}D^+$	0.173665 (46)	0.153342 (45)
$^{79}Br{-}C{\equiv}C{-}H^+$	0.137794 (37)	0.121351 (36)
$^{81}Br{-}C{\equiv}C{-}H^+$	0.137327 (38)	0.121032 (38)
$^{79}Br{-}C{\equiv}C{-}D^+$	0.125767 (29)	0.111312 (29)
$^{81}Br{-}C{\equiv}C{-}D^+$	0.125152 (33)	0.110772 (33)
$I{-}C{\equiv}C{-}H^+$	0.10959 (7)	0.09669 (7)
$I{-}C{\equiv}C{-}D^+$	0.10044 (8)	0.08899 (8)
	B_0 $\tilde{X}^2\Pi$	$\tilde{A}^2\Pi$
$H{-}(C{\equiv}C)_2{-}H^+$	0.14690 (4)	0.14009 (4)
$D{-}(C{\equiv}C)_2{-}D^+$	0.12762 (5)	0.12203 (5)

[a] The references to the studies are given in the text. The values in brackets correspond to one standard deviation.

4. STIMULATED EMISSION PUMPING

The most recent addition to the armoury of spectroscopic techniques available to probe cations is stimulated emission pumping (Kittrell *et al.* 1981). Previously, this approach has been used in the study of highly vibrationally excited levels of closed-shell molecules in their ground electronic state in a static environment (Hamilton *et al.* 1986). It has now been demonstrated that one can also apply this to transient species, such as ions, generated in much smaller concentrations in flow systems (Celii *et al.* 1986*b*).

The ion used to test the feasibility of this approach was the diacetylene cation, for which the $\tilde{A}^2\Pi_u \leftrightarrow \tilde{X}^2\Pi_g$ transition is reasonably well characterized (*vide supra*). In figure 7 are depicted the optical pumping schemes. In one experiment (figure 7*a*) the pump laser (*ca.* 0.08 cm^{-1} band-width) transferred the population to the lowest vibrational level of the $\Omega = \frac{3}{2}$ component of the $\tilde{A}^2\Pi_u$ state whereas the second dye laser (*ca.* 0.25 cm^{-1} band-width) stimulated the transitions to the $\nu_3'' = 1$ and $\nu_7'' = 2$ levels of the $\tilde{X}^2\Pi_{\frac{3}{2},g}$ state. The spectrum obtained can be seen in the left-hand trace of figure 8. The excitation of the degenerate ν_7'' mode in two quanta results in two vibronic components (for the $\Omega = \frac{3}{2}$ substate). In a higher resolution measurement (figure 7*b*), the resolution of the dump laser was increased to *ca.* 0.04 cm^{-1} and the recorded spectrum (figure 8*a*) shows features that are band heads. This is because the excitation laser frequency was tuned to correspond to the R-branch heads and consequently *ca.* 6–10 rotational

PHILOSOPHICAL TRANSACTIONS OF THE ROYAL SOCIETY A MATHEMATICAL, PHYSICAL & ENGINEERING SCIENCES

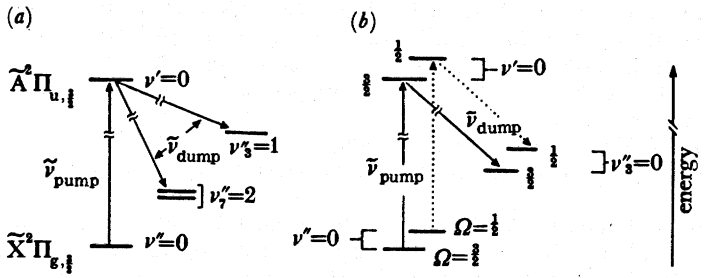

FIGURE 7. Transitions between the ground and excited electronic state of diacetylene cation involved in the stimulated emission pumping experiments.

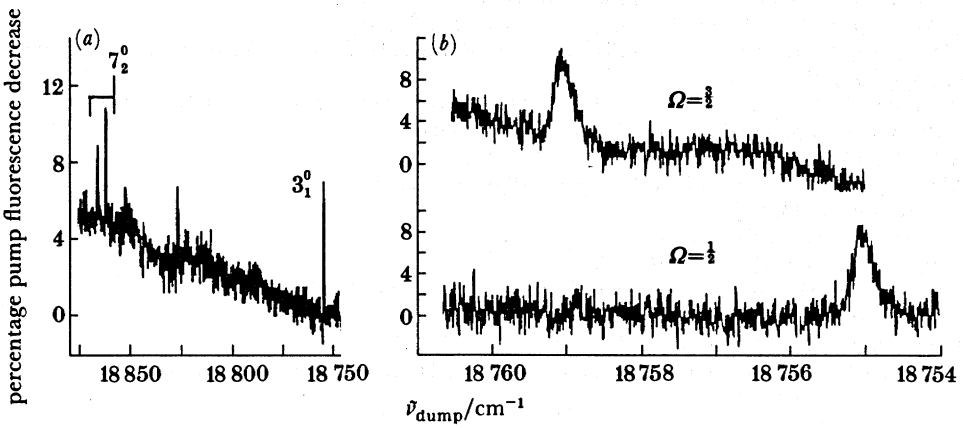

FIGURE 8. Stimulated emission pumping transitions of diacetylene cation (see figure 7) observed (*a*) at low resolution (0.25 cm^{-1}), and (*b*) at higher resolution (0.04 cm^{-1}).

levels (around $J = 25.5$) are populated in either the $\Omega = \frac{1}{2}$ or $\Omega = \frac{3}{2}$ component of the $\tilde{A}^2\Pi_u$ state. As a matter of fact, the assignment of the features in the region of the 3_1^0, 7_2^0 transitions was not clear in the emission spectrum (Callomon 1956); the double-resonance nature of the stimulated emission pumping experiment proves which peaks belong to the 3_1^0 (figure 8*b*) and which belong to the 7_2^0 transition.

A method now exists for probing the ground state of the cations in selected vibrational levels at high resolution to complement such studies in the excited electronic state accessible by the established laser excitation approach.

The research studies described here were realized because of the efforts of the various co-workers whose names are given in the references to the respective studies. The project is financed by the Schweizerischer Nationalfonds zur Förderung der wissenschaftlichen Forschung (no. 2.429-0.84).

REFERENCES

Allan, M. & Maier, J. P. 1976 *Chem. Phys. Lett.* **41**, 231.
Allan, M., Kloster-Jensen, E. & Maier, J. P. 1977 *J. chem. Soc. Faraday Trans.* II **73**, 1406.
Callomon, J. H. 1956 *Can. J. Phys.* **34**, 1046.
Celii, F. G., Fulara, J., Maier, J. P. & Rösslein, M. 1986*a* *Chem. Phys. Lett.* **131**, 325.
Celii, F. G., Maier, J. P. & Ochsner, M. 1986*b* *J. chem. Phys.* **85**, 6230.

Celii, F. G., Rösslein, M., Hanratty, M. A. & Maier, J. P. 1988 *Molec. Phys.* (In the press.)
Fulara, J., Klapstein, D., Kuhn, R. & Maier, J. P. 1985 *J. phys. Chem.* **89**, 4213.
Hamilton, C. E., Kinsey, J. L. & Field, R. W. 1986 *A. Rev. phys. Chem.* **37**, 493.
Hanratty, M. A., Maier, J. P. & Rösslein, M. 1988 (In preparation.)
Herzberg, G. 1971 *Rev. chem. Soc.* **25**, 201.
Herzberg, G. 1985 *Proc. Indian natn. Sci. Acad.* A **51**, 495.
King, M. A., Klapstein, D., Kroto, H. W., Kuhn, R., Maier, J. P. & Nixon, J. F. 1984*a* *J. chem. Phys.* **80**, 2332.
King, M. A., Klapstein, D., Kroto, H. W., Maier, J. P. & Nixon, J. F. 1982 *J. molec. Struct.* **80**, 23.
King, M. A., Klapstein, D., Kuhn, R., Maier, J. P. & Kroto, H. W. 1985*a* *Molec. Phys.* **56**, 871.
King, M. A., Kroto, H. W., Nixon, J. F., Klapstein, D., Maier, J. P. & Marthaler, O. 1981 *Chem. Phys. Lett.* **82**, 543.
King, M. A., Kuhn, R. & Maier, J. P. 1986 *J. Phys. Chem.* **90**, 6460.
King, M. A., Kuhn, R. & Maier, J. P. 1987 *Molec. Phys.* **60**, 867.
King, M. A., Maier, J. P., Misev, L. & Ochsner, M. 1984*b* *Can. J. Phys.* **62**, 1437.
King, M. A., Maier, J. P. & Ochsner, M. 1985*b* *J. chem. Phys.* **83**, 3181.
Kittrell, C., Abramson, E., Kinsey, J. L., McDonald, S. A., Reisner, D. E., Field, R. W. & Katayama, D. H. 1981 *J. chem. Phys.* **75**, 2056.
Klapstein, D., Maier, J. P. & Misev, L. 1983 In *Molecular ions: spectroscopy, structure and chemistry* (ed. T. A. Miller & V. E. Bondybey), pp. 175–200. New York: North Holland.
Kroto, H. W. 1982 *Chem. Soc. Rev.* **11**, 435.
Kuhn, R., Maier, J. P. & Ochsner, M. 1986 *Molec. Phys.* **59**, 441.
Maier, J. P. 1980 *Chimia* **34**, 219.
Maier, J. P. 1982 *Acct. Chem. Res.* **15**, 18.
Maier, J. P. 1986 *J. electron. Spectrosc.* **40**, 203.
Maier, J. P. & Ochsner, M. 1985 *J. chem. Soc. Faraday Trans.* II **81**, 1587.
McDonald, J. K. & Innes, K. K. 1969 *J. molec. Spectrosc.* **29**, 251.
Miller, T. A. & Bondybey, V. E. 1982 *Appl. spectrosc. Rev.* **18**, 105.
Zare, R. N., Schmeltekopf, A. L., Harrop, W. I. & Albritton, D. L. 1973 *J. molec. Specrosc.* **46**, 37.

Discussion

E. HIROTA (*Institute for Molecular Science, Okazaki, Japan*). I have two questions on halogenated acetylene cations. First, does Professor Maier get any information on the Renner–Teller effect? Second, why did Professor Maier not study the fluorinated species? We have investigated the HCCO radical which is an isoelectronic molecule of $HC{\equiv}CF^+$, by microwave spectroscopy. We found the radical to be nonlinear and to have a low-lying electronic state.

J. P. MAIER. We have not studied the Renner–Teller effects in the optical spectra of the haloacetylene cations. The $\tilde{A}^2\Pi \leftrightarrow \tilde{X}^2\Pi$ electronic transitions of $XCCH^+$ and $XCCX^+$, X = Cl, Br, I, have been observed both in emission and by laser excitation. We have analysed the main vibrational features of the spectra, but have not looked into vibronic intractions in any detail; the emission spectra in particular are complex. We have, however, studied such interactions in the $^2\Pi$ ground state of the triatomic cations HBS^+, DBS^+, HCP^+ and DCP^+, as outlined in my paper.

As far as the fluorinated species are concerned, the electronic spectra of $FCCH^+$ and $FCCF^+$ have not been investigated. On the basis of the photoelectron spectra, one may observe the $\tilde{A}^2\Pi - \tilde{X}^2\Pi$ transitions around 200 nm. In the case of $FCCCN^+$, fluorescence from the lowest excited electronic states could not be detected, whereas the $\tilde{A}^2\Pi_g \rightarrow \tilde{X}^2\Pi_u$ emission spectrum of $FCCCCF^+$ has been observed and vibrationally analysed.

G. DUXBURY (*Department of Physics and Applied Physics, University of Strathclyde, Glasgow, U.K.*). I wish to draw attention to the use of methods for calculating the Renner–Teller coupling

PHILOSOPHICAL TRANSACTIONS OF THE ROYAL SOCIETY A MATHEMATICAL, PHYSICAL & ENGINEERING SCIENCES

in triatomic molecules (Jungen & Merer 1980; Duxbury & Dixon 1981) for modelling the isotopic dependence of rotation constants and vibronic parameters. Recently, Lew & Groleau (1987) have completed their analysis of the emission spectrum of D_2O^+. In table D1, the $D_2O^+(\tilde{X}, {}^2B_1)$ constants, calculated by using the parameters derived by Jungen *et al.* (1980) from a fit to the H_2O^+ spectrum are compared with those derived from the analysis of the D_2O^+ spectrum. It can be seen that the degree of agreement is very good. From the calculated values of $A^{SO}_{v,k}$ plotted in figure D1 it can be seen that the sawtooth pattern of the spin–orbit

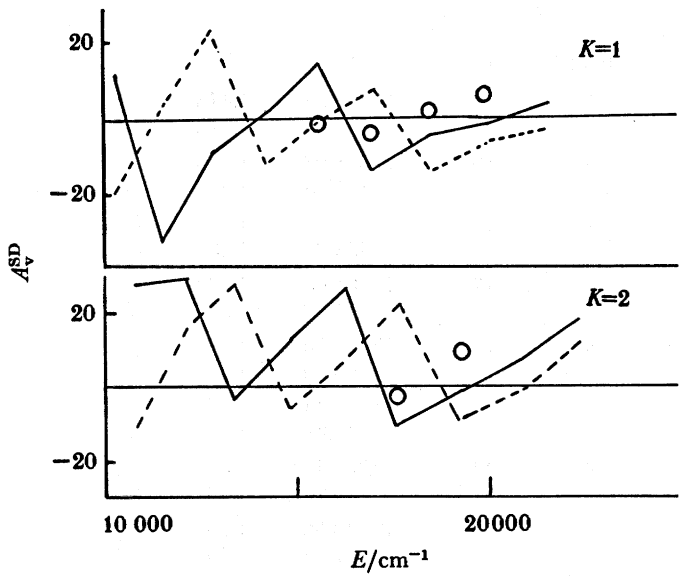

FIGURE D1. Spin–orbit splitting for vibronic levels of the excited state of D_2O^+ with $K = 1$–2. Broken line, calculated as in (*b*), table D1; solid line, calculated as in (*c*), table D1.

TABLE D1. ROTATIONAL CONSTANTS (RECIPROCAL CENTIMETRES) OF THE $\tilde{X}$, $^2B_1$ STATE OF D_2O^+

	$v_2'' = 0$	$v_2'' = 1$	$v_2'' = 2$	$v_2'' = 3$	
A	16.0325	17.6955		22.496	(*a*)
	15.86	17.48	19.71	22.63	(*b*)
	15.84	17.68	20.17	23.52	(*c*)
B	6.2399	6.2624		6.310	(*a*)
	6.212	6.220	6.220	6.218	(*b*)
	6.203	6.193	6.173	6.153	(*c*)
C	4.4066	4.3538		4.224	(*a*)
	4.373	4.317	4.263	4.211	(*b*)
	4.373	4.318	4.265	4.214	(*c*)
ϵ_{aa}	−0.586	−0.782		−1.487	(*a*)
	−0.65	−0.80	−1.01	−1.34	(*b*)
	−0.68	−0.84	−1.10	−1.50	(*c*)
G_0	0.0	1044.27		3058.66	(*a*)
	0.0	1036.81	2044.89	3025.45	(*b*)
	0.0	1044.13	2054.40	3032.20	(*c*)

(*a*) Observed (Lew & Groleau 1987).
(*b*) Calculated (Jungen *et al.* 1980).
(*c*) Calculated as (*b*) except $H'' = 8648\ cm^{-1}$ and $f''_m = 30553.90\ cm^{-1}\ rad^{-2}$.

coupling constants is very sensitive to the upper-state – lower-state splitting pattern. The second calculation with an adjusted ground-state potential barrier can be seen to give good qualitative agreement with the data. The vibronic origins listed in table D2 are also in good agreement. To achieve better quantitative agreement it would be necessary to carry out a simultaneous fit to the data on both isotopic species.

TABLE D2. VIBRONIC CONSTANTS (RECIPROCAL CENTIMETRES) FOR THE LEVELS OF THE $\tilde{A}$, $^2A_1$ STATE OF D_2O^+

K	V bent	V linear	T_v	B_v	
0	5	11	15882.32	4.478	(*a*)
			845.09	4.426	(*b*)
	6	13	17331.93	4.478	(*a*)
			341.76	4.453	(*b*)
	7	15	18807.28	4.468	(*a*)
			833.38	4.480	(*b*)
	8	17	20301.03	4.638	(*a*)
			344.93	4.507	(*b*)
1	4	10	15156.86	4.88	(*a*)
			92.60	4.42	(*b*)
	5	12	16596.14	4.57	(*a*)
			577.91	4.55	(*b*)
	6	14	18057.18	4.55	(*a*)
			45.70	4.48	(*b*)
	7	16	19540.39	4.45	(*a*)
			547.75	4.50	(*b*)
2	5	13	17300.22	4.466	(*a*)
			286.29	4.45	(*b*)
	6	15	18706.91	4.55	(*a*)
			761.32	4.48	(*b*)
3	4	12	16541.38	4.72	(*a*)
			570.10	4.47	(*b*)
	5	14	17989.62	4.57	(*a*)
			984.03	4.49	(*b*)

(*a*) Observed.
(*b*) Calculated as in (*c*) table D1.

The isoelectronic molecules CH_2 and NH_2^+ possess a $^3B_1(^3\Sigma)$ ground state with a low-lying singlet state, $^1A_1$, which forms the lower component of a pair that correlate with $^1\Delta$ of linear $CH_2(NH_2^+)$. Recently experiments have been done on CH_2 to measure the magnetic activity in the singlet system Petek *et al.* (1987). This magnetic activity can result from two causes, residual orbital angular momentum associated with the $^1\Delta$ state, and singlet–triplet mixing. In this discussion I am concentrating on the first of these, angular momentum associated with the linear molecule delta state.

For the dihydrides NH_2 and H_2O^+, a comprehensive study by Jungen & Merer (1980) has shown that the effects of orbital angular momentum can be seen in the erratic variation for small to large, regular or inverted, of the spin–orbit coupling constants of the vibronic levels. This behaviour is associated with the combination of large-amplitude bending vibrational

motion with Renner–Teller coupling between the two states, $^2B_1$ and $^2A_1$, which correlate with the $^2\Pi$ state of linear NH_2. In the NH_2 and H_2O^+ this spin–orbit coupling constant $A^{SO}_{v,k} = A^{SO}\langle\hat{L}_z\rangle$. For a Π state, the maximum value of $\langle\hat{L}_z\rangle = 1$. For CH_2 the maximum value of $\langle\hat{L}\rangle = 2$. However, as the linear molecule limit is $^1\Delta$, there is no spin–orbit interaction constant. The g value of the ro-vibronic levels will be related to the expected value of the orbital angular momentum, i.e.

$$g_{\text{eff}}(K, J) = -K/J\langle\hat{L}_z\rangle = g_r^a K^2/J,$$

where

$$g_r^a = \langle L_z\rangle/K.$$

Christian Jungen and I have recently calculated the variation of $\langle L_z\rangle$ in the singlet levels of CH_2. The result for $K = 1$ is shown in figure D2. It can be seen that the levels recently studied by the Berkeley group, labelled in the figure by M (Petek *et al.* 1987), are those that should show only small effects, and hence most of the magnetic activity observed is because of singlet–triplet mixing.

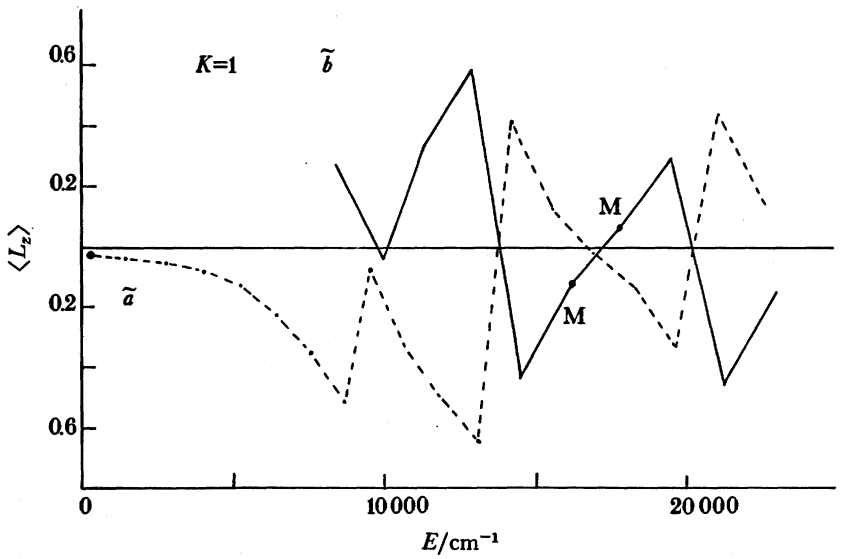

FIGURE D2

Singlet–triplet mixing will, however, depend upon $\langle L_z\rangle$, and our next task is to evaluate explicitly the effects of $\langle L_z\rangle$ on the rate of intersystem crossing. Although NH_2^+ has not been studied in the same detail (Dunlavey *et al.* 1980; Gibson *et al.* 1985), once high-resolution spectra become available similar effects of orbital angular momentum should be shown.

References

Dunlavey, S. J., Dyke, J. M., Jonathan, N. & Morris, A. 1980 *Molec. Phys.* **39**, 1121–1135.
Duxbury, G. & Dixon, R. N. 1981 *Molec. Phys.* **43**, 255–274.
Gibson, S. T., Greene, J. P. & Berkowitz, J. 1985 *J. chem. Phys.* **83**, 4319–4328.
Jungen, Ch., Hallin, K. E. J. & Merer, A. J. 1980 *Molec. Phys.* **40**, 25–94.
Jungen, Ch. & Merer, A. J. 1980 *Molec. Phys.* **40**, 1–24.
Lew, H. 1976 *Can. J. Phys.* **54**, 2028–2049.
Lew, H. & Groleau, R. 1987 *Can. J. Phys.* (Submitted.)
Petek, H., Nesbitt, D. J., Darwin, D. C. & Moore, C. B. 1987 *J. chem. Phys.* **86**, 1172–1188.